LASER-INDUCED INCANDESCENCE FOR SOOT MEASUREMENTS IN TECHNICAL FLAMES AT INCREASED PRESSURE AT THE ONERA M1 TEST RIG

K.P. Geigle, J. Zerbs, Institute of Combustion Technology, DLR,
Pfaffenwaldring 38-40, 70569 Stuttgart, Germany
C. Guin, Department of Fundamental and Applied Energetics, ONERA,
Chemin de la Hunière, 91761 Palaiseau Cedex, France

ABSTRACT

Soot is one of the most discussed pollutants in ground and air traffic. Moreover, its effect as source of intense radiation is significant as soon as local rich mixtures occur, especially at increased pressure. Motivation for soot research is the need to understand soot chemistry for soot formation and oxidation in turbulent, pressurised environment in order to prevent its emission as much as possible. A detailed understanding of the underlying processes can be gained when correlating sophisticated CFD modelling with well defined but yet realistic validation experiments. Within the EU project TLC (Towards Lean Combustion) several experimental tasks are devoted to optimising laser-based diagnostics with ONERA and DLR contributing. One of the contained tasks is dealing with application of laser-induced incandescence (LII) as a tool to determine soot distributions inside the combustor quantitatively. Trends are presented showing soot distributions upon changes of the combustor operating conditions between 4 and 23 bars at realistic geometries and flow rates. In general, the soot concentrations were found to be relatively low. But prior to the final steps of data reduction, interferences from unexpected effects had to be reduced: during the experiments plasma formation at the combustor's base plate, preventing the high power laser beam from exiting the combustor, turned out to be a critical issue. In contrast to the defined LII excitation wavelength at 1064 nm, which can be removed by suitable filtering, the strong resulting broadband plasma radiation was present in the images illuminating combustor walls and flanges. Due to their different dynamics and different statistical behaviour, LII events can be distinguished from plasma radiation; suitable data analysis routines are presented leading to relatively undisturbed soot distributions. The resulting soot average distributions are well suited to determine the positions of soot formation and oxidation as well as quantification of soot concentrations under the highly challenging technical conditions given. Together with data from other tasks (OH and kerosene distributions), studied by ONERA, an excellent validation data set will be available for soot modellers, while the respective industry partners receive a good impression of the low emission capability of their combustor.

1 INTRODUCTION

Soot emission from industrial combustors and engines has a major detrimental impact on air quality and human health, and is now being recognised as potential key factor in global warming. Moreover, its effect as source of intense radiation is significant as soon as local rich mixtures occur, especially at increased pressure. One of the high priorities of manufacturers in cooperation with research is to reduce the environmental impact of soot formation and improve the technology of these industrial combustors. In order to achieve that, a deeper understanding of the physical and chemical mechanisms governing soot formation and oxidation in flames is necessary. The success in modelling soot production in practical aero-engine combustors depends to a large extent on the correct description of mixing as stated in [1]. In the complex flow field prevailing in such combustors, the size and location of fuel-rich regions as sources of soot depend on fuel placement, vaporisation and mixing. A highly sensitive indicator of those fuel-rich regions is the spatially and temporally resolved soot distribution. Laser-based measuring techniques are found to be appropriate for quantification and characterization of particulate emissions. Laser-induced incandescence (LII) in special is a technique that offers many advantages and unique capabilities for the characterisation of soot distributions in combustion [7].

Nomenclature	Pressure [bar]	T(air,in) [K]	ϕ (global)	ϕ (pilot)
Idle, 7% ICAO	4	470	0.2	0.2
Approach, 30% ICAO	9.5	590	0.264	0.12
Cruise-Var1	16.5	590	0.36	0.065
Cruise-Var2	16.5	670	0.36	0.065
Cruise	16.5	670	0.36	0.036
85% ICAO	20	725	0.4	0.054

Table 1: Operating conditions of the studied technical combustor; ϕ(pilot) is contained in ϕ(global), i.e. for *idle*, main injection is not employed.

Recently, technologies have improved rapidly making technical combustion processes accessible by laser optical diagnostics. Applying laser-based methods to realistic combustors offers the opportunity to directly visualise those processes and use the experimental data for validation purposes provided the boundary conditions are well defined. Both approaches promote the understanding of soot chemistry under technical conditions. On the other hand, technical combustion conditions represent a real challenge to the application of laser diagnostics. Measurements have been performed up to 23 bars and data acquisition as well as reduction and quantification are described in detail in the following sections. Finally, soot distributions for standardised ICAO (International Civil Aviation Organization) conditions and similar operating conditions are presented.

2 EXPERIMENTAL SETUP

2.1 Test rig

The test rig infrastructure at the ONERA Palaiseau M1 test facility provides a maximum air flow rate of 3 kg/s at up to 30 bars. Air preheat is possible up to 850 K. For the described experiments, a maximum pressure of 23 bars with 1.6 kg/s air at 725 K preheat temperature were applied. Fuel staging (pilot and main) was provided by the fuel nozzle described below. Operating conditions covered the ICAO conditions *idle*, *approach*, *cruise* and "*85% ICAO*" as well as some others used for trend studies (Table 1).

2.2 Combustion Chamber

The spray flame fed by the fuel nozzle is stabilised inside a combustion chamber having a 105 mm x 105 mm squared cross section and a length of 82 mm before converging to the combustor exit. As typical for swirl stabilised flames, the flame is relatively short due to the intense mixing provided by the swirl and exhibits an inner and an outer recirculation zone. Large quartz windows are used, withstanding pressures up to 30 bars and typical flame temperatures. Their maintenance is provided by a strong film cooling: 26% of the total combustor air flushes the windows' inner surface. Laser sheets can be introduced through a 70 mm x 30 mm window while two windows of 70 mm x 60 mm can be used for detection. With increasing heat release of the studied flames, typically beyond 10 bars, the combustor windows smoothly start to glow, but without exhibiting irreversible damages or interfering with the optical diagnostics. The required chamber pressure is generated by a movable water-cooled piston that is partially blocking the combustor exit.

2.3 Injector

In the studied technical fuel nozzle kerosene can be injected either axially (pilot) through an air blast nozzle or radially through circumferential fuel holes (main). Both fuel flows are separately controlled. While the two inner swirled air flows serve to atomise the pilot fuel (see Fig. 1) the main fuel is multi-point-injected

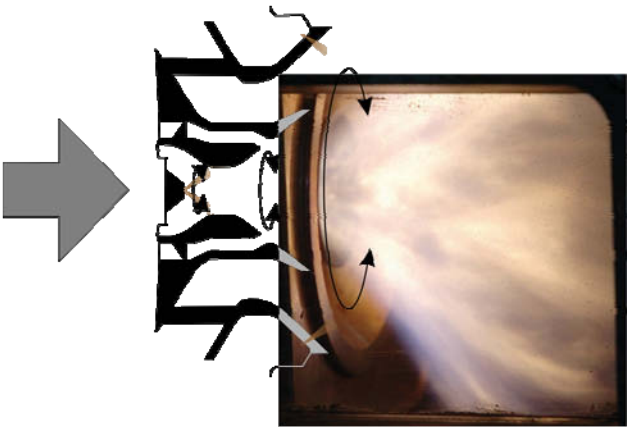

Fig. 1: Schematic of the fuel injector, including pilot (on the axis) and main (annular) and a picture at moderately rich conditions. Flow is from the left to the right.

directly into the outer swirled air flow. For a visual impression a picture at moderately sooting conditions is implemented into the schematic.

2.4 Laser-Induced Incandescence

The Laser Induced Incandescence technique (LII) is based on heating of primary soot particles from flame temperatures up to the vaporisation temperature by a high-energy laser pulse. The absorbed energy is partially emitted as black body radiation with the intensity maximum shifted to the blue compared to the pure flame emission. Above a threshold value in laser power the LII radiation intensity is approximately independent of the laser fluence. Since the particle size is expected to be distinctly smaller than the wavelength of the exciting light (Rayleigh regime) and approximately spherical primary particles can be assumed, the recorded LII signal is directly proportional to the soot volume fraction. For quantification and determination of the calibration factor an independent measurement is necessary (typically an extinction experiment). A comprehensive discussion of the method and its applications can be found in [7] and references therein.

2.5 Optical setup

The optical setup was distributed over two rooms due to safety issues and is illustrated in Fig. 2. The LII-exciting Nd:YAG laser (Quantel, Brilliant) and diagnostics control were placed in a separate control room while the sheet forming optics as well as the detection devices were positioned close to the combustor. The 10 Hz laser output at 1064 nm was guided to an axis parallel, and approximately 0.5 m above the burner axis with several mirrors. A folded 2 lens optics (f_{cyl} = -80 mm, f_{sph} = 1000 mm) followed by an aperture distributed the laser pulse energy of 40 mJ to a sheet 34 mm high and 250 µm wide. A final mirror deflected the sheet down into the combustor while the residual transmittance through this mirror was used to monitor the laser sheet quality on a beam profiler. Due to the buoyant hot environmental air especially above the combustor, the laser sheet suffered some beam steering induced by thermal gradients. Yet, the sheet quality remained good enough for LII excitation. A comparison of undisturbed and steered sheet (prior to entering the combustor) is displayed in Fig. 3. The laser fluence of 0.47 J/cm^2 varies by approximately +/-25% and was chosen to be above the plateau value of the LII response curve in the whole profile. Perpendicular to the excitation in a plane through the burner axis, one ICCD (Lavision, Flamestar 2) was employed to detect chemiluminescence of thermally excited OH radicals with an appropriate spectral filter around 315 nm and 20 µs gate duration monitoring the reaction zone.

Through the opposite window, a second ICCD (PCO, Dicam Pro) recorded soot luminosity and LII at 450 nm with 60 ns gates each. The camera's double frame option allows determining the flame background 500 ns before the laser pulse, i.e. at exactly the same flame conditions. In spite of being weak in intensity, the first frame contains valuable information about the line-of-sight soot distribution of the flame. Due to the combustor window dimensions, not the complete flame is

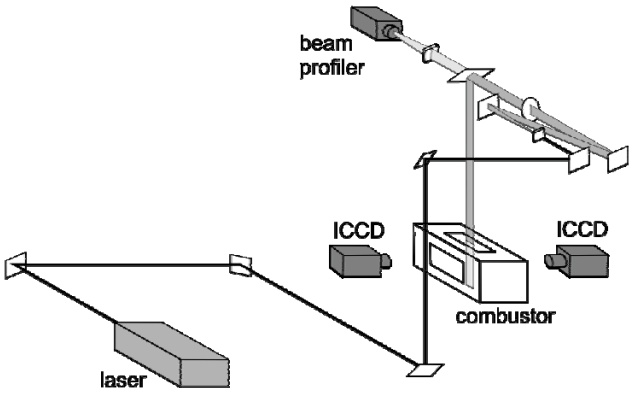

Fig. 2: Optical setup. Laser and combustor are separated by a safety wall.

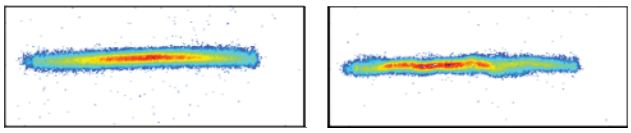

Fig. 3: Beam profile monitored before the laser sheet entering the combustor: before combustor operation (left) and during operation (right).

imaged onto the ICCD cameras. Nevertheless, the full injector outlet plus some additional millimetres are visible on the images, covering a large and important region of the flame. At every operating condition a sequence of 300 single laser shots is recorded with both cameras simultaneously.

In a second measurement, the laser excitation plane was rotated by 90° now being parallel to the burner front panel. In this case a perpendicular detection is impossible. Thus, the camera was oriented relative to the excitation plane by a certain angle while the resulting distortion was corrected for in the data analysis. For this approach only planes close to the injector were accessible.

2.6 Quantification of Laser-Induced Incandescence Images

The highly turbulent flame with its expectedly low soot content of high temporal and spatial fluctuations prohibited an in-situ online calibration with a simultaneous extinction experiment. A suitable stable calibration flame could not be introduced in the position of the measurement due to spatial constraints as for example described in [4,6,9,10]. Alternatively, a calibration experiment was performed ex-situ in the laboratory applying the same LII excitation and detection system in the same geometry with similar thick combustion chamber windows to a stationary calibration flame, similar to [8]. An additional extinction experiment at 1064 nm was used to provide absolute soot concentrations over the extinction pathway that were correlated with a respective LII image. For absorption, a wavelength of 1064 nm was chosen rather than a shorter wavelength [4,8] since here the contribution of PAH to the total absorption can be neglected [3].

2.7 Detection interferences

Spray scattering interferences of the exciting laser into the LII detection window were not to be expected [2,9] due to the difference in

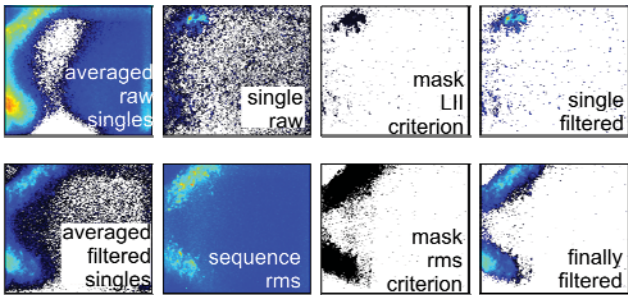

Fig. 4: Procedure of correcting time-averaged LII images for scattered plasma light; details are explained in the text.

excitation and detection wavelengths. Another interference turned out to be more severe. Opposite of the combustor window used to introduce the laser sheet an instrumentation flange was mounted. Sufficiently close to the laser focus, white plasma was generated on the metal surface that was scattered into the LII camera by combustion chamber and window flange surfaces. Due to its broadband character, a spectral discrimination was not successful. Instead, a suitable filtering mechanism was implemented into the data analysis procedure, removing large parts of this interference. The filtering routine is based on the completely different behaviour of scattered plasma light and LII events: while the plasma is generated more or less in the same position every laser shot, only depending on the sheet quality transmitted through the highly turbulent flow, the typically stronger LII events change position and intensity. As a result, plasma scattering remains negligible in the single shot images that are dominated by LII events, if any. In case of too high scattering levels, the filtering routine fails. For the formation of time-averaged images, two different masks were applied: The sequence average only accounts for those events from the single shot images having sufficiently enough signal and spatial dimension (mask LII). That excludes areas of low, homogeneously distributed scattering as well as background

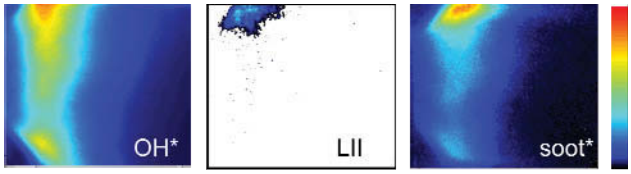

Fig. 5: Correlation of laser-induced and passive diagnostics at *cruise* condition: LII (centre), OH chemiluminescence (left), soot emission (right) all show asymmetrical flame behaviour.

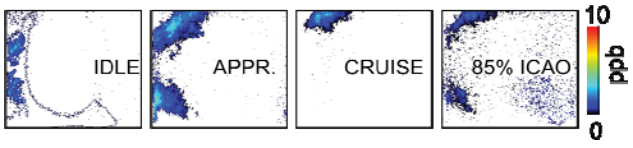

Fig. 6: Spatially resolved, time-averaged soot distributions for defined ICAO conditions.

noise. High dynamics of the LII events are expressed in the rms image of a sequence of 300 single laser pulses. Here, plasma scattering is characterised by moderate values, in contrast to LII events. The rms image is used as a second filter to the sequence averages, removing intensity from positions where too low intensity fluctuations occur (mask rms). The complete procedure is illustrated in Fig. 4.

3 RESULTS

In all following representations, flames burn from left to right. Fig. 5 illustrates the advantage of laser excited emission diagnostics as the central image, laser-induced incandescence, represents the time-averaged soot distribution in the plane of laser excitation. In contrast to the line-of-sight diagnostics, namely OH chemiluminescence and soot emission, it can be quantified as displayed below. Both line-of-sight images at this operating condition (*cruise*) show a certain asymmetry of the flame, as frequently detected in swirl flames that are sensitive to various influence parameters of a combustor, for example buoyancy. While the OH* image shows a more diffuse species distribution, the soot emission is rather localised and fits well to the spatially resolved LII distribution. Concentrations of both species drop to very low values within the monitored area, even faster in the case of soot, that is oxidised to values below the sensitivity of the detection device. The short flame length monitored by both species correlates well to the visual impression and expectations for a swirl flame.

In the next Fig. 6 the time-averaged soot distribution from *cruise* conditions (Fig. 5) is complemented by three other ICAO standard conditions: *idle*, *approach* and "*85% ICAO*". The soot distribution is not in all cases comparably asymmetric as at *cruise* conditions.

For the *idle* representation it must be noticed that strong combustor window pollution occurred during the measurements, mainly due to the low air temperature and smaller mass flows inducing worse mixing. The introduced

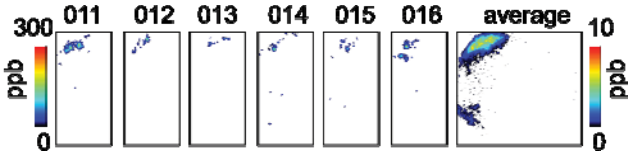

Fig. 7: Comparison of subsequent single shot soot distributions (colour bar for quantification on the left) and time averaged soot distribution (colour bar on the right) for combustor condition Var2.

contour line represents the limit of soot luminosity dropping to zero; in the central part of the combustor window soot on the inner window surface prevented signal transmission, similarly visible in the OH* image as detected through the opposite combustor window and visually from the control room. This effect was not observed for the other displayed flames. All conditions presented in this figure exhibit very low and similar averaged soot concentrations at ppb level. Downstream soot concentrations drop below the sensitivity level of the detection system or disappear out of the optically accessible regions; the corresponding images excited in a second laser sheet position are not shown as signal is negligible. With one respect, the *idle* condition differs from the others: the detected soot distribution is located relatively close to the combustor axis due to the full fuel injection through the pilot. The other operating conditions are characterised by decreasing pilot injection to zero resulting in soot formation at larger radial position.

Another indication of weakly sooting conditions is visible in Fig. 7 showing a good injector performance with respect to soot formation. This figure shows several subsequent single shot images (quantified colour bar on the left) compared to the averaged image on the right (with a separate colour bar). The single shot images are characterised by relatively small, mostly pointwise soot events of temporally and spatially highly statistical behaviour. Several single shots of a sequence do not show

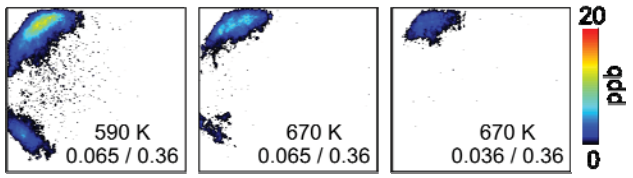

Fig. 8: Influence of air inlet temperature on soot formation (left to centre, Var1 and Var2) and fuel distribution at constant global ϕ (centre to right); right is *cruise*. Note the different colour bar relative to Fig. 7.

any LII signal. For strongly sooting flames, soot events are expected to be chained, wrinkled, linked, and finally surrounded by large homogeneous low concentration soot fields. The statistical behaviour finds its expression in the peak values up to 0.3 ppm, a still relative low value, while the average of 300 images is even below 10 ppb.

Fig. 8 shows the trend of soot formation at different air inlet temperature for constant fuel injection (left and centre image). While in principle soot formation should be kinetically controlled and thus augment at increased temperature. This behaviour is found for prevaporised kerosene combustion [5]. In contrast, the effect is counter-balanced in kerosene spray flames since increased temperature accelerates vaporisation of the spray followed by improved mixture and reduction of locally rich Shifting the fuel injection from pilot towards main at constant global equivalence ratio (Fig. 8, centre to right, right is *cruise*) reduces soot production while soot formation occurs more lifted from the nozzle. Distribution of the fuel through multi-holes rather than through the central pilot optimises the mixture under these operating conditions, thus reducing local fuel-rich spots and soot formation.

Regarding the planes parallel to the burner front panel (Fig. 9) indicates a circular, donut shaped soot field on average, increasing in diameter with distance from the burner as expected from the perpendicular view (Fig. 6). The horizontal shadows are due to starting cracks on the pressure windows or local window pollution preventing the laser from entering the combustor. Again, certain asymmetries of intensity are visible following the argumentation presented above. However, as already demonstrated above, soot concentrations increase with distance from the injector. Close to the burner axis and in the corner recirculation zones no soot is detected. The remaining fine-structure in these sequence-

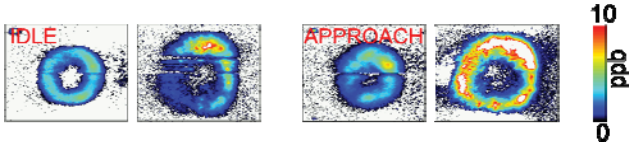

Fig. 9: Soot concentrations in planes parallel to the burner front plate for idle and approach, at 4 mm (first and third plot) and 13 mm distance (second and fourth plot), respectively.

averaged images is correlated to the still insufficient number of single shot images acquired per sequence. Yet it is a good compromise between statistic evidence and duration of the measurements. Note that larger structured signatures with more stable locations, as for example OH PLIF, can easily provide significantly smoother images. In general, those images provide a good complement of the planes including the combustor axis.

4 SUMMARY

Laser-induced incandescence has successfully been applied to a spray combustor at technical conditions, covering some of the ICAO operating points and variations of the main operating parameters. Maximum operating pressure during the tests was 23 bars while this paper describes results between 4 and 20 bars. Interferences from scattered plasma light induced by the laser focus on the combustion chamber surface were removed from the images during data analysis. Averaged LII images are compared to pure emission images monitoring OH* and soot emission. For quantification of LII a stable premixed flame at ambient pressure was employed and LII correlated with a line-of-sight extinction experiment at 1064 nm while using the same optical setup as in the technical experiment. This approach is known to bias soot volume fractions determined for high pressures towards too small values but appeared to be the only feasible. Nevertheless, soot concentrations determined under the defined technical conditions remained clearly below 1 ppm peak in single shot images and even one order of magnitude lower in averages over 300 single shots using the described calibration. Thus, the used spray injector showed a very good performance with respect to soot emissions even when keeping in mind the given uncertainties at high pressure. Consideration of the measured soot structures confirms this statement additionally. Together with OH and kerosene PLIF experiments performed by another team [11] a comprehensive data set at highly technical conditions is established that can be used for validation of simulation tools.

5 ACKNOWLEDGEMENT

Funding of the work by the European Community under the Sixth Framework Programme, Aeronautics and Space, project TLC - Towards Lean Combustion Contract N°AST4-CT-2005-012326 is gratefully acknowledged. Additionally, special thanks are expressed for the excellent support of the test campaign by J.J Lecout, E. Paux and E. Landais.

6 REFERENCES

[1] H. Brocklehurst, J.B. Moss, C.D. Hurley, C.H. Priddin, Soot and Radiation Modelling in Gas Turbine Combustion Chambers, RTO Meeting Proceedings 14, Gas Turbine Engine Combustion, Emissions and Alternative Fuels (1999).

[2] J.E. Dec, A.O. zur Loye, D.L. Siebers, Soot Distribution in a D.I. Diesel Engine Using 2-D Laser-Induced Incandescence Imaging, SAE Tech. Paper 910224 (Society of Automotive Engineers), Warrendale, Pa. (1991).

[3] J. Zerbs, K.P. Geigle, O. Lammel, J. Hader, R. Stirn, R. Hadef, W. Meier, The influence of wavelength in extinction measurements and beam steering in laser-induced incandescence measurements in sooting flames, Appl. Phys. B 96 (2009), 683-694.

[4] O. Lammel, K.P. Geigle, R. Lückerath, W. Meier, and M. Aigner, Investigation of Soot Formation and Oxidation in a High-Pressure Gas Turbine Model Combustor by Laser Techniques, Proc. ASME Turbo Expo, Montreal (Canada), GT2007-27902 (2007).

[5] U. Meier, C. Hassa, K.P. Geigle, O. Lammel, P. Kutne, Parametric Study of Soot Formation in an Aeroengine Model Combustor at Elevated Pressures by Laser-Induced Incandescence: Effect of the Fuel Phase, Proc. First CEAS European Air and Space Conference, Berlin, Paper 233 (2007).

[6] J.A. Pinson, D.L. Mitchell, R.J. Santoro, T. A. Litzinger, Quantitative, Planar Soot Measurements in a D.I. Diesel Engine Using Laser-Induced Incandescence and Light Scattering, SAE Tech. Paper 932650 (Society of Automotive Engineers), Warrendale, Pa. (1993).

[7] R.J. Santoro, C.R. Shaddix, in: K. Kohse-Höinghaus, J.B. Jeffries (Eds.), Applied Combustion Diagnostics. Taylor & Francis, New York, 2002, pp. 252.

[8] M.S. Tsurikov, K.P. Geigle, V. Krüger, Y. Schneider-Kühnle, W. Stricker, R. Lückerath, R. Hadef, M. Aigner, Laser-Based Investigation of Soot Formation in Laminar Premixed Flames at Atmospheric and Elevated Pressures, Combust. Sci. Technol. 177 (2005) 1835-1862.

[9] R.L. Vander Wal, D.L. Dietrich, Laser-Induced Incandescence Applied to Droplet Combustion, Appl. Opt. 34 (1995) 1103-1107.

[10] G. Wiltafsky, W. Stolz, J. Köhler, C. Espey, The Quantification of Laser-Induced Incandescence (LII) for Planar Time Resolved Measurements of the Soot Volume Fraction in a Combusting Diesel Jet, SAE Tech. Paper 961200 (Society of Automotive Engineers), Warrendale, Pa. (1996).

[11] F. Grisch, M. Orain, B. Rossow, E. Jourdanneau, C. Guin, Simultaneous equivalence ratio and flame structure measurements in multipoint injector using PLIF, Proc. 44th AIAA/ASME/SAE/ASEE Joint Propulsion Conference & Exhibit, Hartfort, CT, AIAA 2008-4868 (2008).